Nuclear Theory'21
ed. V. Nikolaev, Heron Press, Sofia, 2002

Y-Scaling Analysis of the Deuteron within the Light-Front Dynamics Method

M.K. Gaidarov, M.V. Ivanov, and A.N. Antonov

Institute of Nuclear Research and Nuclear Energy, Bulgarian Academy of Sciences, Sofia 1784, Bulgaria

Abstract.

The concept of relativistic scaling is applied to describe the most recent data from inclusive electron-deuteron scattering at large momentum transfer. We calculate the asymptotic scaling function $f(y)$ of the deuteron using its relationship with the nucleon momentum distribution. The latter is obtained in the framework of the relativistic light-front dynamics (LFD) method, in which the deuteron is described by six invariant functions f_i (i=1,...,6) instead of two (S and D waves) in the nonrelativistic case. Comparison of the LFD asymptotic scaling function with other calculations using S and D waves corresponding to various nucleon-nucleon potentials, as well as with the Bethe-Salpeter result is made. It is shown that for $|y| > 400$ MeV/c the differences between the LFD and the nonrelativistic scaling functions become larger.

1 Introduction

High-energy electron scattering from nuclei can provide important information on the wave function of nucleons in the nucleus. In particular, using simple assumptions about the reaction mechanism, scaling functions can be deduced that, if shown to scale (i.e., if they are independent of the momentum transfer), can provide information about the momentum and energy distribution of the nucleons. Several theoretical studies [1–5] have indicated that such measurements may provide direct access to studies of short-range nucleon-nucleon (NN) correlation effects.

Since West's pioneer work [6], there has been a growth of interest in y-scaling analysis, both in its experimental and theoretical aspects. This is motivated by the importance of extracting nucleon momentum distributions from the experimental

data. West showed that in the impulse approximation, if quasielastic scattering from a nucleon in the nucleus is a dominant reaction mechanism, a scaling function $F(y)$ could be extracted from the measured cross section which is related to the momentum distribution of the nucleons. In the simplest approximation the corresponding scaling variable y is the minimum momentum of the struck nucleon along the direction of the virtual photon. In principle, the scaling function $F(y, Q^2)$ depends on both y and momentum transfer Q^2 (-Q^2 is the square of the four-momentum transfer), but at sufficiently high Q^2 values the dependence on Q^2 should vanish yielding scaling. However, any attempt to extract the momentum distribution from the y-scaling in electron-nucleus scattering faces the problem of estimating both effects from the final-state interactions (FSI) of the struck nucleon with the rest of the nucleus and from the nucleon binding. Previous calculations [7–9] suggest that the contribution from the final-state interactions should vanish at sufficiently high Q^2. The FSI lead to sizable scaling violation effects only at low values of the three-momentum transfer $|\mathbf{q}| = \sqrt{Q^2 + \nu^2}$ (ν is the energy loss) [9,10]. The most important dynamical effects, such as binding corrections, which represent the fact that for complex nuclei the final spectator $A - 1$ system can be left in all possible excited states including the continuum, have been treated in [2] in terms of spectral functions. This problem has been solved in [11, 12] by introducing a new scaling variable which gives direct, global and independent of A link between the experimental data and the longitudinal momentum components.

Recently inclusive electron scattering has been studied at the Thomas Jefferson National Accelerator Facility (TJNAF) with 4.045 GeV incident beam energy from C, Fe and Au targets [13] to $Q^2 \approx 7$ (GeV/c)^2. Data were also taken using liquid targets of hydrogen and deuterium [14]. The data presented in [13, 14] represent a significant increase of the Q^2 range compared to previous SLAC measurement [15], in which an approach to the scaling limit for heavy nuclei is suggested but for low values of $|y| < 0.3$ GeV at momentum transfers up to 3 (GeV/c)^2, and, moreover, a scaling behaviour is observed for the first time at very large negative y (y= -0.5 GeV/c). From theoretical point of view the extended region of y measured at TJNAF is of significant importance since this is a regime where the nucleon momentum distribution is expected to be dominated by short-range NN correlations. On the other hand, it is interesting to note that contributions from short-range FSI may also result in a scaling-like behavior due to the small Q^2 dependence of these effects, and that these contributions are also dominated by short-range correlations. Obviously, a complete understanding of this electron-nucleus scattering requires a relativistic approach to the quantities related to the y-scaling analysis for a detailed comparison with the experimental data.

A relativistic y-scaling has been considered in [16] by generalizing the nonrelativistic scaling function to the relativistic case. Realistic solutions of the

spinor-spinor Bethe-Salpeter (BS) equation for the deuteron with realistic interaction kernel were used for systematic investigation of the relativistic effects in inclusive quasielastic electron-deuteron scattering. The approach of y-scaling presented in [16] is fully covariant, with the deuteron being described by eight components, namely the ${}^3S_1^{++}$, ${}^3D_1^{++}$, ${}^3S_1^{--}$, ${}^3D_1^{--}$, ${}^1P_1^{+-}$, ${}^1P_1^{-+}$, ${}^3P_1^{+-}$, and ${}^3P_1^{-+}$ waves. The first two waves directly correspond to the S and D waves in the deuteron, with the waves with negative energy vanishing in the nonrelativistic limit. It has been demonstrated in [16] that, if the effects from the negative energy P-states are disregarded, the concept of covariant momentum distribution can be introduced.

Recently a successful relativistic description of the nucleon momentum distribution in deuteron has been done [17] within the light-front dynamics method [18,19]. The most important result from the calculations in [17] is the possibility of the LFD method to describe simultaneously both deuteron charge form factors (that has been shown in [20]) and the momentum distribution. It is shown in [19,21] that after the projection of the Bethe-Salpeter amplitude on the light front, the six components of the LFD deuteron wave function are expressed through integrals over the eight components of the deuteron Bethe-Salpeter amplitude. Provided the nucleon-nucleon interaction is the same, these approaches incorporate by different methods the same relativistic dynamics. The wave functions in LFD are the direct relativistic generalization of the nonrelativistic ones in the sense that they are still the probability amplitudes. Therefore they can be used in the relativistic nuclear physics (e.g. [18]).

The aim of our work is using the nucleon momentum distribution $n(k)$ obtained with the LFD method to calculate the deuteron scaling function. The result for the asymptotic function is compared with the recent TJNAF data measured at six values of Q^2. In particular, the scaling behavior observed for very large negative y providing momenta higher than those corresponding to existing experimental data for $n(k)$ may allow to distinguish the properties of the covariant LFD method from the potential approaches. The comparison with the BS result for the scaling function serves as a test for the consistency of both covariant approaches treating the deuteron relativistically in the case of y-scaling.

The paper is organized as follows. In Section 2 the definition and the physical meaning of the scaling variable and the scaling function are briefly reviewed together with some basic relations between the nucleon spectral function, the scaling function and the momentum distribution. The results for the nucleon momentum distribution in deuteron obtained within the LFD method are given in Section 3. The calculated LFD asymptotic scaling function of the deuteron is presented in Section 4, where a comparison with the Bethe-Salpeter result and with some nonrelativistic calculations is also done. The summary of the present work is given in Section 5.

2 Basic Relations in the y-Scaling Method

The scaling function is defined as the ratio of the measured cross section to the off-shell electron-nucleon cross section multiplied by a kinematic factor:

$$F(q,y) = \frac{d^2\sigma}{d\Omega d\nu}(Z\sigma_p + N\sigma_n)^{-1}\frac{q}{[M^2+(y+q)^2]^{1/2}},$$

where Z and N are the number of protons and neutrons in the target nucleus, respectively, σ_p and σ_n are the off-shell cross sections, and M is the mass of the proton. In analysing quasielastic scattering in terms of the y-scaling a new variable $y = y(q,\nu)$ is introduced. Then the nuclear structure function which is determined using the spectral function $P(k,E)$ as

$$F(q,\nu) = 2\pi\int_{E_{min}}^{E_{max}(q,\nu)} dE \int_{k_{min}(q,\nu,E)}^{k_{max}(q,\nu,E)} kdkP(k,E), \qquad (1)$$

can be expressed in terms of q and y rather than q and ν (see Eq. (1)). In Eq. (1) $E = E_{min} + E^*_{A-1}$ is the nucleon removal energy with E^*_{A-1} being the excitation energy of the final $A-1$ nucleon system.

The most commonly used scaling variable y is obtained [22] starting from relativistic energy conservation, setting $k = y$, $\frac{\mathbf{kq}}{kq} = 1$ and the excitation energy E^*_{A-1}=0, and is defined through the equation

$$\nu + M_A = (M^2 + q^2 + y^2 + 2yq)^{1/2} + (M^2_{A-1} + y^2)^{1/2}, \qquad (2)$$

where M_A is the mass of the target nucleus and M_{A-1} is the mass of the $A-1$ nucleus. Therefore, y represents the longitudinal momentum of a nucleon having the minimum removal energy ($E = E_{min}$, i.e. E^*_{A-1}=0).

At high values of q a pure scaling regime is achieved, where $k_{min} \approx |y - (E - E_{min})|$ and Eq. (1) becomes

$$F(q,y) \to f(y) = 2\pi\int_{E_{min}}^{\infty} dE \int_{|y-(E-E_{min})|}^{\infty} kdkP(k,E). \qquad (3)$$

In Eq. (3) the particular behavior of $P(k,E)$ at large k and E is used in order to extend the upper limits of integration to infinity [2].

In the deuteron one always has E^*_{A-1}=0, so that the spectral function is entirely determined by the nucleon momentum distribution $n(k)$, i.e. $P(k,E) = n(k)\delta(E-E_{min})$, and, consequently, $k_{min} = |y|$ for any value of q. The scaling function (3) reduces to the longitudinal momentum distribution

$$f(y) = 2\pi\int_{|y|}^{\infty} k\, dk\, n(k). \qquad (4)$$

3 Nucleon Momentum Distribution in the Light-Front Dynamics Method

The relativistic deuteron wave function (WF) on the light-front $\Psi(\vec{k},\vec{n})$ depends on two vector variables: i) the relative momentum $\vec{k}$ and ii) the unit vector $\vec{n}$ along $\vec{\omega}$ which determines the position of the light-front surface. Due to this, the WF is determined by six invariant functions f_i (i=1,...,6) instead of two (S- and D-waves) in the nonrelativistic case. Each one of these functions depends on two scalar variables k and $z = cos(\widehat{\vec{k},\vec{n}})$. In LFD these six functions are calculated within the relativistic one-boson-exchange model. As shown in [18], in the nonrelativistic limit the functions f_{3-6} become negligible, $f_{1,2}$ do not depend on z and turn into S- and D-waves ($f_1 \approx u_S$, $f_2 \approx -u_D$) and the wave function $\Psi(\vec{k},\vec{n})$ becomes the usual nonrelativistic wave function. One of the most important properties of the functions f_{1-6} found in [18] is that for $k \geq 2 \div 2.5$ fm^{-1} the component f_5 (being related mainly to π-exchange) exceeds sufficiently the S- and D-waves. This fact is very important in the calculations of $n(k)$ in deuteron as it will be shown below.

The LFD calculations have shown (for more details, see Ref. [17]) that, as expected, the most important contributions to the total $n(k)$ give terms related to the f_1, f_2 and f_5 functions

$$n(k) \simeq n_1(k) + n_2(k) + n_5(k). \tag{5}$$

The contributions of n_1, n_2, $n_{12} = n_1 + n_2$ and n_5 are compared in Figure 1. It can be seen that, while the functions f_1 and f_2 give a good description of the

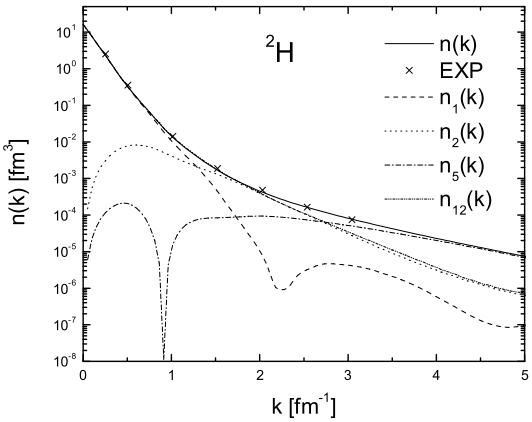

Figure 1. The nucleon momentum distribution in deuteron. The contributions of n_1, n_2, $n_{12} = n_1 + n_2$ and n_5 are presented. The y-scaling data are from [2]. The normalization is: $\int n(k) d^3\vec{k} = 1$.

y-scaling data of $n(k)$ for $k < 2$ fm^{-1} (like the S- and D-wave functions in the nonrelativistic case), it is impossible to explain the high-momentum components of $n(k)$ at $k > 2$ fm^{-1} without the contribution of the function f_5. We note that the deviation of the total $n(k)$ from the sum $n_{12} = n_1 + n_2$ starts at k around 1.8 fm^{-1}. All this shows the important role of NN interactions which incorporate exchange of relativistic mesons in the case of the deuteron.

The nucleon momentum distribution in the deuteron using S- and D-wave functions $\Psi_S(k)$ and $\Psi_D(k)$ corresponding to various NN potentials, such as the charge-dependent Bonn potential [23], the Argonne v_{18} [24], the Nijmegen - I ,- II and - Reid 93 [25] and Paris 1980 [26] is also computed in [17] by the expression:

$$n(k) = \frac{1}{4\pi}[\Psi_S^2(k) + \Psi_D^2(k)] \equiv n_S(k) + n_D(k) \tag{6}$$

with

$$\int n(k) d^3\vec{k} = 1\,. \tag{7}$$

In Figure 2 the result for $n(k)$ using the charge-dependent Bonn potential [23] is given and compared with the y-scaling data. As can be seen, the D-component of $n(k)$ is important but even its inclusion does not give a very good agreement with the data for $k \geq 2$ fm^{-1}. In the next Figure 3 we present the LFD result for $n(k)$ compared with the calculations using the WF's corresponding to Nijmegen-I,-II, -Reid 93, Argonne v_{18} and Paris 1980 NN potentials and with the y-scaling data. We would like to note that: i) the results of the calculations

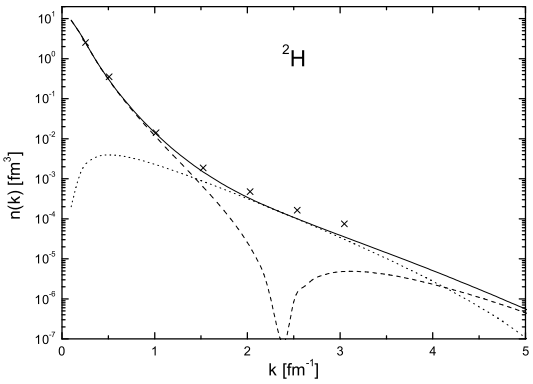

Figure 2. The nucleon momentum distribution in deuteron (solid line) calculated using Eqs. (6) and (7) with S- and D-wave functions corresponding to the charge-dependent Bonn potential [23]. S- and D-contributions are given by dashed and dotted line, respectively. The y-scaling data are from [2].

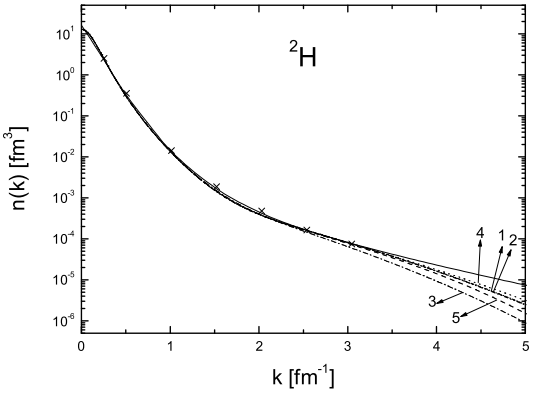

Figure 3. The nucleon momentum distribution in deuteron calculated with the LFD (solid line) in comparison with the results presented by numerated arrows, as follows: 1-Argonne v_{18}, 2-Nijmegen Reid 93, 3-Nijmegen I, 4-Nijmegen II, 5-Paris 1980 NN potentials and with the y-scaling data [2].

using the NN potentials, such as Nijmegen-II, -Reid 93, Argonne v_{18} and Paris 1980 (shown in Figure 3) are in better agreement with the y-scaling data than those using the charge-dependent Bonn potential (Figure 2). This might be related to the fact that these potentials describe NN phase shifts up to larger energies (e.g. the Nijmegen-II potential gives reasonable pp phase shifts up to 1.2 GeV, while the charge-dependent one-boson exchange Bonn potential fits the phase-shift data below 350 MeV); ii) It can be seen from Figure 3 that there are small differences between the curves corresponding to different NN potentials for $k \leq 3$ fm^{-1} (which give a good description of the y-scaling data and almost coincide with the LFD result) and larger ones for $k > 3$ fm^{-1}. Large differences take place, however, between all of them and the LFD result for $k > 3$ fm^{-1}.

4 Results for the Asymptotic Scaling Function of Deuteron

In this Section we present the results for the asymptotic scaling function of deuteron which is calculated by using of the LFD nucleon momentum distribution given in Section 3.

The scaling function for deuteron calculated within the LFD method is shown in Figure 4. It is compared with the TJNAF experimental data [14] for all measured angles. The Q^2 values are given for Bjorken $x = Q^2/2M\nu = 1$ and correspond to elastic scattering from a free nucleon. It is seen from Figure 4 that the relativistic LFD scaling function is in good agreement with the data in the whole region of negative y available. As known, the scaling breaks down for values of $y > 0$ due to the dominance of other inelastic processes beyond the quasielastic

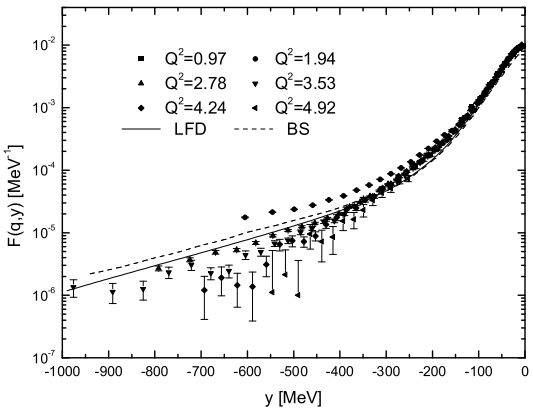

Figure 4. The scaling function of deuteron. The experimental data for different Q^2 values are from [14]. The solid and dashed curves represent the LFD calculations of this work and BS result of Ref. [16].

scattering. Our LFD deuteron scaling function is also compared in Figure 4 with the scaling function obtained within the BS formalism [16]. A small difference between the two results is observed for $y < -400$ MeV/c but, at the same time, the theoretical LFD scaling function is closer to the experimental data in the same region of y. The fact that both LFD and BS functions reveal similar behavior is a strong indication in favor of the consistency of the two relativistic covariant approaches in case of the y-scaling.

In Figure 5 the asymptotic relativistic LFD and BS scaling functions $f(y)$ are compared with the nonrelativistic ones, calculated with some realistic interactions. We have already shown (see Figures 2 and 3 of the present work) that the results using these potentials explain very well (with the exception of the charge-dependent Bonn potential) all the available data for $n(k)$ up to $k \simeq 3$ fm^{-1} exactly like the LFD method. However, it is concluded in [17] that for $k > 3$ fm^{-1} the LFD results for $n(k)$ deviate strongly from those of the calculations using NN potentials. Here we would like to emphasize the existence of the same discrepancies between the scaling functions observed from the comparison in Figure 5. It is shown that for $|y| > 400$ MeV/c both LFD and BS curves start to deviate from the nonrelativistic scaling functions. The result for $f(y)$ calculated using the Nijmegen-II NN potential is in better agreement with the experimental data than those using other potentials. It is in accordance with the result for $n(k)$ shown in Figure 3. For instance, by a thorough comparison between the relativistic Bethe-Salpeter and the nonrelativistic scaling functions of deuteron it has been found in [16] that the two functions start to sensibly differ also at $|y| > 400$ MeV/c. Thus, the necessity to treat realistically the relativistic dynamics inside the deuteron in a way different from the potential approaches becomes apparent.

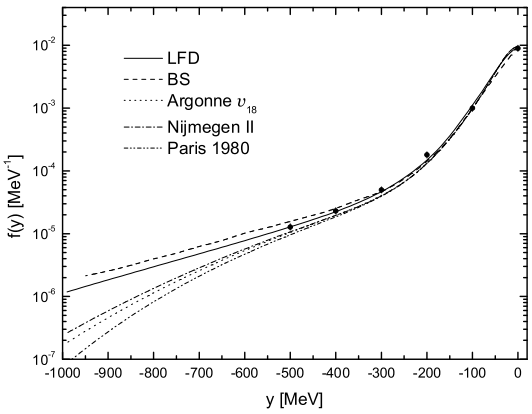

Figure 5. The asymptotic scaling function of deuteron. Line convention refering to calculations using LFD and potential approaches, as well as BS result [16] is given (see also the text). The experimental data [27] are given by the full circles.

In this sense, the results calculated for both momentum distribution and asymptotic scaling function confirm the abilities of the LFD method to describe with a good accuracy the experimental data measured at high momentum transfers.

5 Conclusions

In the present paper inclusive electron-deuteron scattering data have been analyzed in terms of the y-scaling function within the light-front dynamics method. For this purpose, the nucleon momentum distribution in deuteron has been used in order to calculate the asymptotic scaling function. For the trivial case of deuteron, for which the structure function (Eq. (3)) coincides with the longitudinal momentum distribution (Eq. (4)) we have found a good agreement of the calculated scaling function with the experimental data. Thus, the concept of relativistic y-scaling can be introduced in the LFD relativistic description of inclusive quasielastic eD scattering, in the same way as it is done in the conventional nonrelativistic approach, i.e. by introducing a scaling function (which, in the scaling regime, is nothing but the nucleon longitudinal momentum distribution), and in terms of the same variable y. It has been pointed out that for $|y| > 400$ MeV/c the differences between the LFD and the nonrelativistic scaling functions are very large.

Exploring the light-front dynamics, we continue in this paper our analysis of important deuteron characteristics. The effective inclusion of the relativistic nucleon dynamics and of short-range NN correlations can be better seen when analyzing electron scattering at high momentum transfer from complex nuclei, for which a proper theoretical y-scaling analysis is still lacking. Although scal-

ing violation effects due to final-state interactions sharply decrease with increasing momentum transfer, a consistent treatment of both FSI and nucleon binding must be made in order to perform a precise comparison with the new TJNAF data. Such an investigation is in progress.

Acknowledgments

This work was partly supported by the Bulgarian National Science Foundation under the Contracts Nrs.Φ–809 and Φ–905.

References

[1] Xiangdong Ji and J. Engel, (1989) *Phys. Rev.* **C40** R497.

[2] C. Ciofi degli Atti, E. Pace, and G. Salmè, (1991) *Phys. Rev.* **C43** 1155.

[3] C. Ciofi degli Atti and S. Simula, (1994) *Phys. Lett.* **B325** 276.

[4] C. Ciofi degli Atti and S. Simula, (1996) *Phys. Rev.* **C53** 1689.

[5] M.K. Gaidarov, A.N. Antonov, S.S. Dimitrova, and M.V. Stoitsov, (1995) *Int. J. Mod. Phys.* **E4** 801.

[6] G.B. West, (1975) *Phys. Rep.* **18** 263.

[7] O. Benhar, A. Fabrocini, S. Fantoni, G.A. Miller, V.R. Pandharipande, and I. Sick, (1991) *Phys. Rev.* **C44** 2328.

[8] O. Benhar and V.R. Pandharipande, (1993) *Phys. Rev.* **C47** 2218.

[9] C. Ciofi degli Atti, L.P. Kaptari, and D. Treleani, (2001) *Phys. Rev.* **C63** 044601.

[10] C. Ciofi degli Atti, E. Pace, and G. Salmè, (1987) *Phys. Rev.* **C36** 1208.

[11] C. Ciofi degli Atti and G.B. West, (1999) *Phys. Lett.* **B458** 447.

[12] D. Faralli, C. Ciofi degli Atti, and G.B. West, (2000) *Proceedings of 2nd Int. Conf. on Perspectives in Hadronic Physics, ICTP, Trieste, Italy , 10-14 May 1999*, (eds. S. Boffi, C. Ciofi degli Atti, and M.M. Giannini; World Scientific, Singapore) p.75.

[13] J. Arrington *et al.*, (1999) *Phys. Rev. Lett.* **82** 2056.

[14] J. Arrington, (1998) *PhD Thesis*.

[15] D.B. Day *et al.*, (1987) *Phys. Rev. Lett.* **59** 427.

[16] C. Ciofi degli Atti, D. Faralli, A.Yu. Umnikov, and L.P. Kaptari, (1999) *Phys. Rev.* **C60** 034003.

[17] A.N. Antonov, M.K. Gaidarov, M.V. Ivanov, D.N. Kadrev, G.Z. Krumova, P.E. Hodgson, and H.V. von Geramb, (2002) *Phys. Rev.* **C65** 024306.

[18] J. Carbonell and V.A. Karmanov, (1995) *Nucl. Phys* **A581** 625.

[19] J. Carbonell, B. Desplanques, V.A. Karmanov, and J.-F. Mathiot, (1998) *Phys. Rep.* **300** 215 (and references therein).

[20] D. Abott *et al.*, Jefferson Lab. t_{20} Collaboration, (2000) *Phys. Rev. Lett.* **84** 5053.

[21] S. Bondarenko, V.V. Burov, M. Beyer, and S.M. Dorkin, (1999) *Few-Body Systems* **26** 185.

[22] E. Pace and G. Salmè, (1982) *Phys. Lett.* **B110** 411.

[23] R. Machleidt, (2001) *Phys. Rev.* **C63** 024001.

[24] R.B. Wiringa, V.G.J. Stoks, and R. Schiavilla, (1995) *Phys. Rev.* **C51** 38.

[25] V.G.J. Stoks, R.A.M. Klomp, C.P.F. Terheggen, and J.J. de Swart, (1994) *Phys. Rev.* **C49** 2950.

[26] M. Lacombe, B. Loiseau, J.M. Richard, R. Vinh Mau, J. Côté, P. Pirès, and R. de Tourreil, (1980) *Phys. Rev.* **C21** 861.

[27] D. Day *et al.*, (1990) *Annu. Rev. Nucl. Part. Sci.* **40** 357.